ELSEVIER

Journal of Organometallic Chemistry 579 (1999) 164–176

Journal of Organometallic Chemistry

# Interaction of oxygen functionalized alkenes with a methylaluminoxane–zirconocene catalyst studied by NMR

Tuulamari Helaja [a,*], Kimmo Hakala [b], Juho Helaja [a], Barbro Löfgren [b]

[a] *Department of Chemistry, PO Box 55, University of Helsinki, FIN-00014 Helsinki, Finland*
[b] *Polymer Science Center, Helsinki University of Technology, PO Box 356, FIN-02150 Espoo, Finland*

Received 28 September 1998

**Abstract**

Reactions of hydroxyl, ether and carbonyl functionalized alkenes with methylaluminoxane prepared in toluene-$d_8$ (MAO) and zirconocenedichloride ($Cp_2ZrCl_2$) were investigated by $^1$H- and $^{13}$C-NMR spectroscopy at 27°C. The 11 alkenes studied bear a terminal C=C bond separated by 7–9 ($-CH_2-$) units from the heteroatom moiety. Intramolecular connectivities in mono (alkene), bi (alkene and MAO) and tri (alkene, MAO and $Cp_2ZrCl_2$) component mixtures were determined by 2D HSQC, HMBC, ROESY and NOESY NMR techniques. The five studied alkenols formed aluminium alkoxides with MAO even in the case of a substantial steric hindrance around the OH group. Zirconocene enhanced the formation of aluminium alkoxides. Decomposition to free alkenol was observed only for the straight chain alkenol (10-undecen-1-ol). The OTMS derivatives formed dimers of the type $CH_2{=}CR_1R_2$ along with methyl derivatives, $CH_2{=}C(Me)(R)$ and $(Me)CH{=}CH(R)$, in the presence of MAO and $Cp_2ZrCl_2$. 10-Undecenyl methyl ether and methyl decenoate remained mainly as a free comonomer in the presence of MAO or MAO/$Cp_2ZrCl_2$, though a transient coordination of the former to MAO was deduced. Unsaturated species $Me_2C{=}CH-Al-X$ and $CH_2{=}CH(CH_2)_5CH_2CH{=}C(t\text{-Bu})O-Al-X$ (X = MAO oligomer) were formed in the reaction of *t*-butyl undecenoate or 2,2-dimethyl-11-dodecen-3-one with MAO or MAO/$Cp_2ZrCl_2$. Interaction of the $CH_2{=}CH$ part of the functionalized alkenes with zirconocene was not observed. A possible coordination of the C=C bond to MAO was observed only for the *sec* alkenols. © 1999 Elsevier Science S.A. All rights reserved.

*Keywords:* Functionalized alkenes; Zirconocene–methylaluminoxane catalyst; NMR

## 1. Introduction

The structural features of MAO and its oligomeric interconversion have been extensively studied by $^1$H-, $^{13}$C-, $^{17}$O- and $^{27}$Al-NMR [1–6]. It is suggested that residual trimethylaluminium (TMA) in MAO solution participates in the interconversion of linear, branched and cyclic MAO oligomers. In addition to the linear and cyclic oligomers the presence of clusters with three coordinated oxo ligands has been proposed (Scheme 1). The synthesis and structural characterization of cage alumoxanes, $[(t\text{-Bu})Al(\mu_3\text{-O})]_n$ ($n = 6,8,9$), support the latter [7].

The MAO–zirconocene interaction has been monitored by $^1$H-, $^{13}$C-, $^{27}$Al- and $^{91}$Zr-solution NMR [3,8–12] and solid-state XPS [13] or CPMAS [14] techniques.

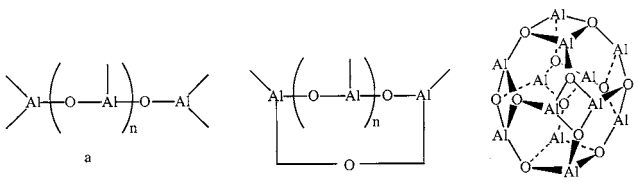


Scheme 1. The suggested structural elements of MAO: (a) linear, (b) cyclic and (c) cage structures (methyl groups have been omitted for clarity) [1,7].

* Corresponding author. Fax: +358-9-1914-0366.
*E-mail address:* tuulamari.helaja@helsinki.fi (T. Helaja)


PII: S0022-328X(98)01219-4

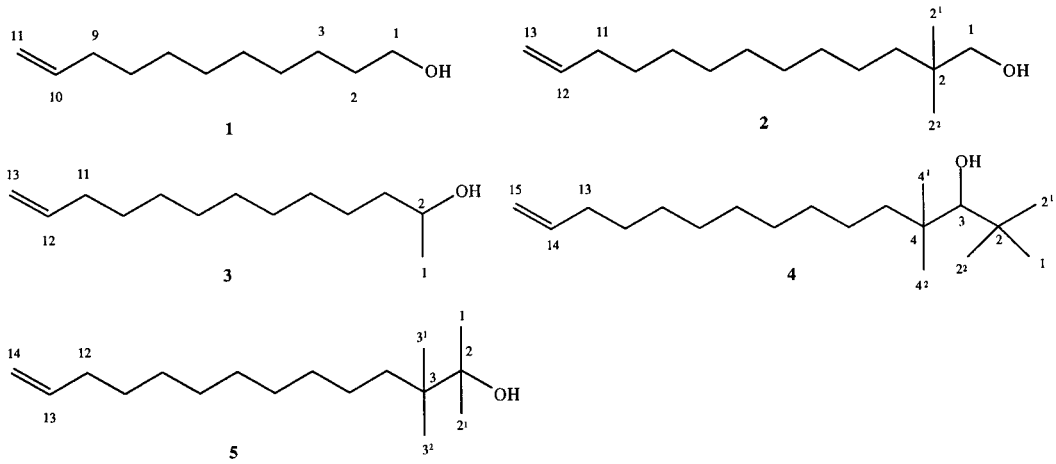


Scheme 2. The structures of alkenols studied: 10-undecen-1-ol (**1**), 2,2-dimethyl-12-tridecen-1-ol (**2**), 12-tridecen-2-ol (**3**), 2,2,4,4-tetramethyl-14-pentadecen-3-ol (**4**) and 2,3,3-trimethyl-13-tetradecen-2-ol (**5**). The numbers refer to the characteristic $^{1}H$ and $^{13}C$ atoms monitored by NMR.

These indicate a formation of a $[Cp_2ZrR]^+$ cation stabilized by an $[R\text{-}MAO]^-$ counterion and a subsequent displacement of the anion by an olefin molecule in polymerization (R = alkyl, Cp = cyclopentadienyl

Table 1
Characteristic chemical shift values ($\delta$, ppm) for mono-, bi- and tri-component mixtures of alkenols **1**–**5** measured in toluene-$d_8$ (multiplicity of the observed $^{1}H$-NMR signal is given in parentheses and the atomic numbers refer to Scheme 2)

| Compound number | Atomic number | Alkenol | | Alkenol with MAO or MAO/$Cp_2ZrCl_2$ | |
|---|---|---|---|---|---|
| | | $^{1}H$ $\delta$ (ppm) | $^{13}C$ $\delta$ (ppm) | $^{1}H$ $\delta$ (ppm) | $^{13}C$ $\delta$ (ppm) |
| **1** | 1 | 3.45 (t) | 62.7 | 4.00 (m) | 64.6 |
| | 2 | 1.40 (m) | 33.3 | 1.90 (bm) | 33.3 |
| **2** | 1 | 3.13 (s) | 71.7 | 3.44 (s) | 73.2 |
| | | | | * 3.58 (s) | * 84.7 |
| | $2^1$, $2^2$ | 0.83 (s) | 24.1 | 0.82 (s) | 24.1 |
| **3** | 1 | 1.05 (d) | 23.8 | 1.14 (d) | 23.3 |
| | 2 | 3.58 (m) | 67.7 | 3.81 (m) | 71.1 |
| | | | | * 3.88 (m) | * 80.5 |
| **4** | 1, $2^1$, $2^2$ | 1.00 (s) | 29.1 | * 1.00 [a] (s) | * 29.1 [a] |
| | | | | * 1.03 [b] (s) | * 29.7 [b] |
| | | | | 1.15[c] (s) | 31.0 [c] |
| | 3 | 2.95 (s) | 83.7 | * 2.95 [a] (d) | * 83.7 [a] |
| | | | | * 3.40 [b] (s) | * 100.1 [b] |
| | | | | 3.66[c] (s) | 92.5[c] |
| | $4^1$, $4^2$ | 0.96 (s) | 25.6 and 26.0 | * 0.96 [a] (s) | n.r. |
| | | | | * 0.98 [b] | n.r. |
| | | | | * 1.01 [b] | n.r. |
| | | | | 1.08 [c] | 26.83 [c,i] |
| | | | | 1.16 [c] | 26.82 [c,i] |
| **5** | 1, $2^1$ | 1.03 (s) | 25.6 | 1.35 [a] | 25.6 [a] |
| | | | | 1.47 [b] | 26.2 [b,ii] |
| | | | | 1.49 [c] | 26.1 [c,ii] |
| | 2 | | 74.9 | | 85.6 [a] |
| | | | | | 86.1 [b,c] |
| | $3^1$, $3^2$ | 0.85 (s) | 21.6 | 0.89 [a] | 22.4 [a] |
| | | | | 0.93 [b] | 22.7 [b,iii] |
| | | | | 0.94 [c] | 22.8 [c,iii] |

* Detected only in the presence of $Cp_2ZrCl_2$.
[a,b] and [c] refer to the different molecular fragments present in the bi- or tri-component mixtures, (i, ii, iii) mutually interchangeable signals, n.r., not resolved.

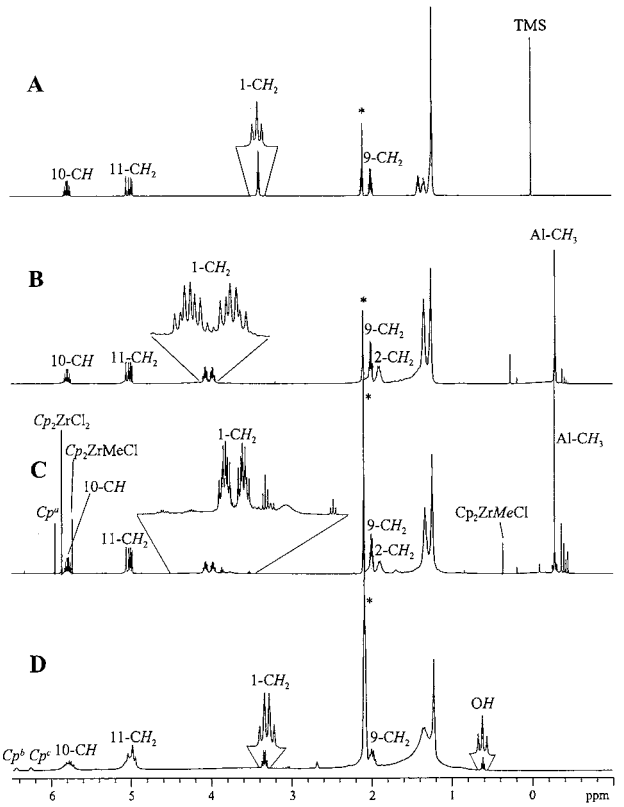


Fig. 1. The $^1$H-NMR spectrum (500 MHz) of (A) **1**, (B) **1** and MAO, (C) **1**, MAO and $Cp_2ZrCl_2$ and (D) aged **1** (300 MHz), MAO and $Cp_2ZrCl_2$ referenced* to the residual $CHD_2$ in toluene-$d_8$. The numbering refers to Scheme 2. Different $Cp_2Zr$ species are marked with superscripts a–c.

ligand). Recently, an ion-pair complex of a cage alumoxane, $[(t\text{-Bu})Al(\mu_3\text{-}O)]_6$, and $Cp_2ZrMe_2$ has been detected and proven to be an active catalyst for ethene polymerization [15].

In addition to the spectroscopic investigations of MAO or MAO–zirconocene interaction, reactions of cage alumoxanes and of related alkylalumoxanes with different heteroatom compounds have been reported [16–19]. However, interaction(s) appearing in a three-component system of the polar comonomer, MAO and zirconocene has not been thoroughly investigated.

We have previously studied the synthesis of functional polyolefins through direct polymerization of ethene or propene and some polar oxygen functionalized comonomers with soluble zirconocene–MAO catalysts [20–23]. The catalyst deactivation was observed to vary depending on the structural features of a polar monomer utilized in the copolymerization.

In the present study, interaction of OH, OR, $CO_2R$ and C=O functionalized long-chain alkenes with MAO prepared [24] in toluene-$d_8$ solution and a $Cp_2ZrCl_2$ catalyst are discussed. The mono (pure alkene)-, bi (alkene/MAO)- and tri (alkene/MAO/$Cp_2ZrCl_2$)-component reaction mixtures were investigated using $^1$H- and $^{13}$C-NMR spectroscopy. Intramolecular connectivities between nuclei have been deduced by HSQC, HMBC, ROESY and NOESY 2D NMR techniques. $^1$H-$^1$H ROESY and NOESY measurements have been further performed to reveal the possible catalyst coordination to the vinyl and/or heteroatom moiety of the comonomer and to have an insight into the spatial vicinity of the protons in the bi- or tri-component systems. Comparison of the NMR and actual ethene or propene copolymerization results is also briefly described.

## 2. Results and discussion

### 2.1. Reactions of alkenols with the MAO–$Cp_2ZrCl_2$ catalyst system

Five hydroxyl functionalized alkenes **1**–**5** (Scheme 2) with varying degrees of steric hindrance around the oxygen atom were allowed to react with the MAO–$Cp_2ZrCl_2$ catalyst system. The interaction(s) between the alkenol and the catalyst system were analyzed by comparing the characteristic $^1$H- and $^{13}$C-NMR resonances of pure alkenol (mono component) to the signals observed for the bi (alkenol and MAO)- and tri (alkenol, MAO and $Cp_2ZrCl_2$)-component mixtures (Table 1).

#### 2.1.1. Primary alkenol *1*

The $^1$H-NMR spectra of compound **1** measured in different component systems are presented in Fig. 1(A–D). The 1-C$H_2$ of free alkenol **1** has the chemical shift value $\delta$ 3.45 ppm (Fig. 1(A)). These protons were shifted to a lower field at $\delta$ 4.00 ppm, when the NMR sample contained an equimolar amount of MAO (Fig. 1(B)). Simultaneously their multiplicity changed from a triplet to a fine-structured doublet presumably due to the unsymmetry induced by different MAO fragments. The chemical shift values and the multiplicity of the observed proton signals remained the same, when a catalytic amount of $Cp_2ZrCl_2$ was added to the mixture of **1** and MAO (Fig. 1(C)). Additional multiplets at $\delta$ 3.50–4.40 ppm, barely visible in the bi-component mixture, became more pronounced in the tri-component mixture of **1**.

On the basis of HSQC spectra the 1-$C$H$_2$ resonance of **1** assigned at $\delta$ 62.7 ppm had shifted ($\Delta\delta$(C) = 1.9 ppm) to an upper value of 64.6 ppm measured in the bi- and tri-component systems. Two HMBC correlations (Fig. 2) between a $^1$H singlet ($\delta$ −0.30 ppm) and 1-$C$H$_2$ or 2-$C$H$_2$ resonances (64.6 and 33.3 ppm) were detected indicating the formation of an aluminium alkoxide. Chemical shift values of −0.35 ppm [2], −0.38 ppm [4] and −0.40 ppm [6] are generally attributed to TMA present as a free dimer ($Al_2Me_6$) or

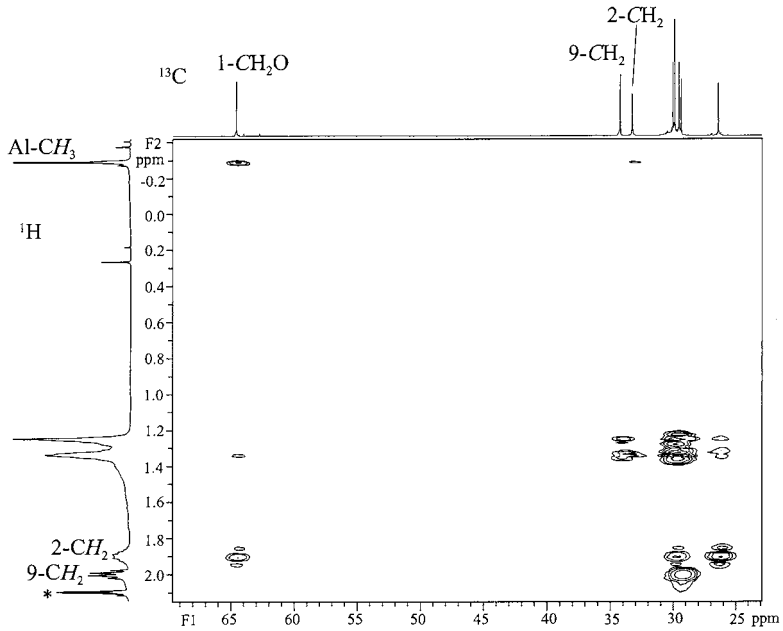


Fig. 2. The expanded HMBC (500 MHz) spectrum of **1** and MAO.

mainly bound to MAO. Alternatively, O–Al($CH_3$)$_2$ chain-end methyl protons of MAO oligomers could appear at $\delta - 0.38$ ppm [4].

We assume that there exists one main aluminium alkoxide and a few minor similar components based on the observed HMBC correlations and the TROESY spectrum measured from the bi- or tri-component mixtures of **1**. The ROE correlations (Fig. 3) arising from the spectral area of 3.50–4.40 ppm to the group of singlets at $\delta$ $-0.26$ to $-0.46$ ppm suggest that compound **1** has reacted with MAO oligomers and thus produced different $RCH_2$–O–Al– fragments, of which the main species could be formed from the residual TMA present in MAO. In that case the main component has most likely a trimeric structure since dimethylaluminium alkoxides, $Me_2Al(OR)$ with straight-chain hydrocarbon substituents (R), have been observed to favor the trimeric form in solution [25].

When the NMR sample containing **1**, MAO and $Cp_2ZrCl_2$ was allowed to stand for a few weeks in the dark, some gelatinous material was formed in the NMR tube. Subsequently, both the $^1$H- and $^{13}$C-NMR spectra had changed significantly. Now a $^1$H resonance with the appearance of a deceptive quartet was detected at $\delta$ 3.36 ppm (Fig. 1(D)). A coupling constant of 5.5 Hz was obtained for the deceptive quartet and the triplet at $\delta$ 0.62 ppm indicating that they are part of the same spin system. Based on the HSQC and HMBC spectra these signals are most likely the 1-C$H_2$ and O$H$ of free alkenol **1**. The assigned OH proton showed distinct HMBC correlations to the 1-$CH_2$, 2-$CH_2$ and 3-$CH_2$ resonances ($\delta$ 62.5, 33.0 and 26.5 ppm) attributable to the values measured for the pure **1**. Hence, the originally formed aluminium alkoxides seem to be unstable under the experimental conditions.

The pronounced effect of aging is also noticed by inspecting the chemical shift values of cyclopentadienyl protons (Cp). Pure $Cp_2ZrCl_2$ has its Cp resonance (s) at $\delta$ 5.88 ppm ($\delta_C$ 116.0 ppm). In the freshly measured tri-component $^1$H-NMR spectrum (Fig. 1(C)), two additional Cp resonances were observed: one at the upper value of 5.95 ppm ($\delta_C$ 113.5 ppm) and the other at the lower value of 5.78 ppm ($\delta_C$ 112.6 ppm). The chemical shift value of 5.74–5.76 ppm has been assigned to the Cp moiety of $Cp_2ZrCH_3Cl$ whereas the $\delta$ value of 0.36–0.43 ppm was obtained for the Zr–$CH_3$ resonance depending on the concentration of MAO [11]. These can both be identified in the $^1$H-NMR spectrum presented in Fig. 1(C). We assume that the upper $\delta$ value (5.95 ppm) is produced by coordination of MAO or TMA aluminium to a chlorine of $Cp_2ZrCl_2$ or $Cp_2ZrCH_3Cl$ on the basis of induced downfield shift ($\Delta\delta_H = 0.07$ ppm compared to $Cp_2ZrCl_2$). These types of complexes have been suggested to occur in a reaction of MAO and $Cp_2ZrCl_2$ [1,8,9,11].

The original Cp signals were absent at the $^1$H spectrum recorded from the aged tri-component mixture (Fig. 1(D)). Two proton resonances (bs) having the $\delta$ values 6.29 and 6.47 ppm ($\delta_C$ 133.5 and 133.0 ppm) were found with a mutual HMBC correlation instead. Such lowfield resonances have been earlier reported for $Cp_2Zr^+(Me)O(CH_2)_nCH{=}CH_2$ ($n = 1$–3) cations with anionic counterions [26]. However, the observed $\delta_C$ values, 133.5 and 133.0 ppm, are not in agreement with

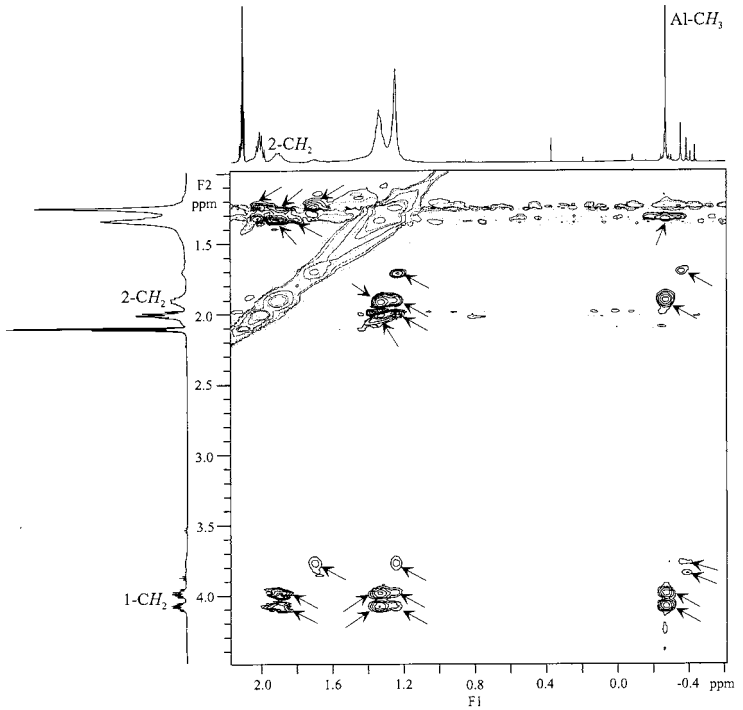


Fig. 3. The expanded TROESY (500 MHz) spectrum of **1** and MAO; correlations are marked with arrows.

the chemical shifts commonly assigned for Cp carbons in $Cp_2Zr^+(R)(L)$ (L = ligand), $Cp_2Zr(OR)_2$ or $Cp_2Zr(R)OR$ [10,26,27]. Presumably the high $\delta_C$ values obtained are due to a substituent attached to the Cp ring. This is supported by the HMBC correlations detected between the resonances at $\delta_H$ 2.70 ppm ($\delta_C$ 41.8 ppm) and $\delta_C$ 133.5 ppm as well as at $\delta_H$ 6.29 ppm and $\delta_C$ 41.8 ppm.

### 2.1.2. Primary and secondary alkenols *2* and *3*

Several partly overlapping –C(Me$_2$)C$H_2$–O– and –C*H*(Me)–O– resonances appeared at $\delta$ 3.40–4.40 ppm, when the NMR spectrum was measured from a mixture of compound **2** or **3** and MAO–$Cp_2ZrCl_2$ (Fig. 4(A–B)). Consequently the geminal *C*–O resonances ($\delta$ 70–85 ppm) from the HSQC spectra could no longer be unequivocally deduced with the exceptions noted in Table 1. HMBC correlations could be observed from the different $2^1/2^2$-C$H_3$ of **2** ($\delta$ 0.80–1.20 ppm) and 1-C$H_3$ of **3** ($\delta$ 1.00–1.25 ppm) to the corresponding 1-*C*–O ($\delta$ 73.0–84.7 ppm) and 2-*C*–O ($\delta$ 71.0–80.5 ppm) signals.

Obviously various –C(Me$_2$)C$H_2$–O– and –C*H*-(Me)–O– species are produced from structurally different MAO oligomers. This is supported by the ROESY spectra of **2** or **3** and the catalyst system. The 1-C$H_2$ resonances of **2** ($\delta$ 3.44–4.10 ppm) showed ROE correlations to the $2^1/2^2$-C$H_3$ signals ($\delta$ 0.80–1.20 ppm). The partly overlapping Al–C$H_3$ resonances centred at $\delta$ −0.40 and −0.38 ppm had ROE correlations to 1-C$H_2$ at $\delta$ 3.44 and 3.70 ppm, respectively.

For compound **3**, ROE correlations from the 2-C*H* signals (br) at $\delta$ 4.14 and 4.28 ppm to the Al–C$H_3$ signals (unresolved) at $\delta$ −0.30 to −0.48 ppm were recorded in the presence of MAO. Additional weak ROE correlations were observed for the mixture of **3**, MAO and $Cp_2ZrCl_2$. The 13-C$H_2$ ($\delta$ 5.00 ppm, m) and 11-C$H_2$ protons exhibited ROE correlations to the Al-C$H_3$ ($\delta$ −0.30 ppm, unresolved) and Al–C$H_3$ (bs, centered at $\delta$ −0.10 ppm), correspondingly.

The Cp signals measured for the tri-component mixtures of **2** or **3** (Fig. 4) appear approximately at the same $\delta$ values as described for compound **1** (Fig. 1(C)). Thus the interaction of the olefinic part of **3** and MAO manifested at the ROESY spectrum is

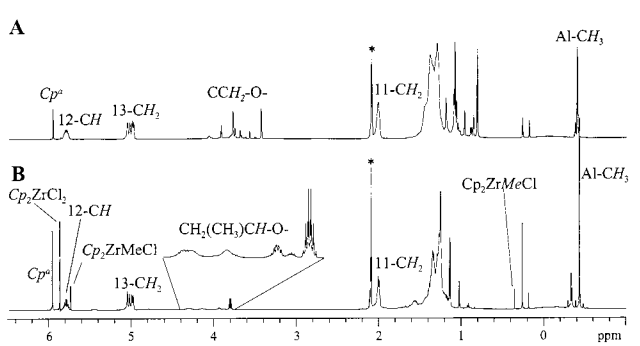


Fig. 4. The $^1$H-NMR spectrum (600 MHz) of (A) **2**, MAO and $Cp_2ZrCl_2$ and (B) **3**, MAO and $Cp_2ZrCl_2$.

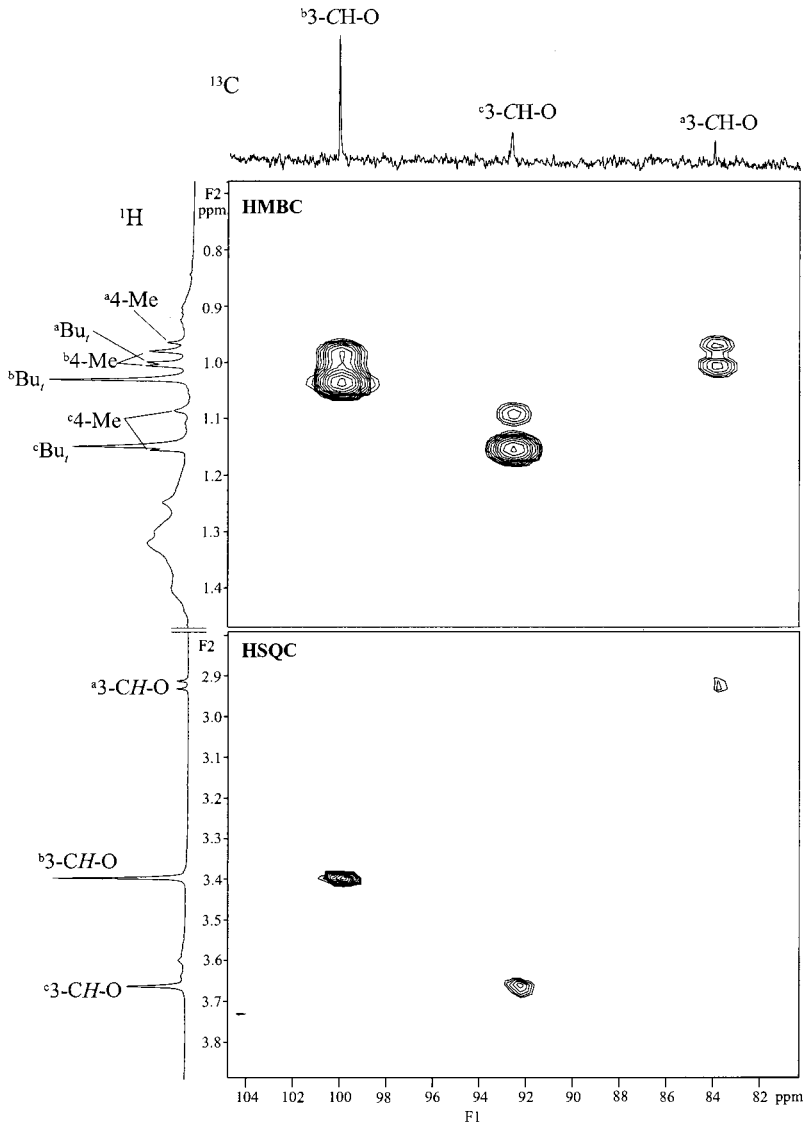


Fig. 5. The expanded HMBC and HSQC spectrum (300 MHz) of aged **4**, MAO and $Cp_2ZrCl_2$.

probably induced by the suitable structure of *sec* alkenol **3** and not by a zirconocene species absent in the reaction mixtures of *prim* alkenol **1** or **2**. Moreover, the decomposition of the formed alkoxides as described for the straight chain alkenol **1** did not occur in the tri-component mixtures of the branched compounds **2** or **3**.

### 2.1.3. Secondary and tertiary alkenols *4* and *5*

Compound **4** represents a *sec* alcohol with a substantial steric hindrance around the oxygen atom. The 3-C*H* (s) resonance for pure **4** was observed at $\delta$ 2.95 ppm. In the bi-component system a single lower field 3-C*H* signal ($\delta$ 3.66 ppm, s) was detected. Obviously the bulky alkyl groups of **4** prevent the OH group from forming the multiple CH–O– species found for the *sec* alkenol **3**. The 3-C*H* ($\delta$ 3.66 ppm) signal showed HMBC correlations to the $^{13}C$ resonances at $\delta$ 40.8 ($C_q$), 38.1 ($C_q$), 31.0 (1-$CH_3$, $2^1$-$CH_3$ and $2^2$-$CH_3$), 26.83, 26.82 ($4^1$-$CH_3$ and $4^2$-$CH_3$) ppm. A $^1H-^1H$ ROE correlation was detected between the 3-C*H* and a $^1H$ triplet ($\delta$ −0.20 ppm, br) supporting the formation of an aluminium alkoxide. The vinyl 15-C$H_2$ of **4** ($\delta$ 5.00 ppm) exhibited a weak ROE correlation to the broad signal of MAO ($\delta$ 0.00 ppm) as described earlier for the tri-component mixture of **3**.

The addition of $Cp_2ZrCl_2$ produced another aluminium alkoxide having its 3-C*H* resonance at $\delta$ 3.40 ppm (Table 1). The originally formed alkoxide ($\delta_H$ 3.66 ppm) and free **4** ($\delta_H$ 2.95 ppm) were detected as well. After keeping the NMR sample for a few weeks in the dark, the intensity ratio 1:1:1 originally observed for the 3-CH protons at $\delta$ 3.66, 3.40 and 2.95 ppm was readjusted to 3:5:1. The analysis of the 2D spectra

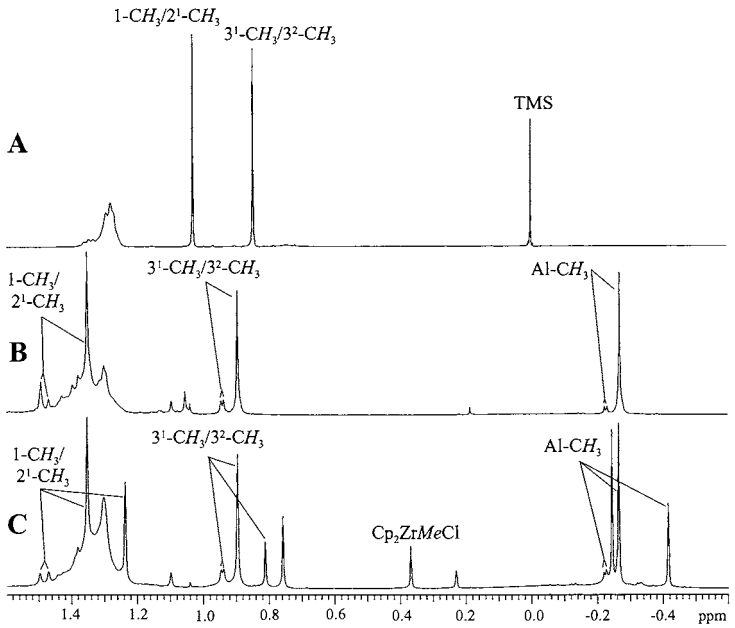


Fig. 6. The expanded $^1$H-NMR spectrum (500 MHz) of (A) **5**, (B) **5** and MAO and (C) (300 MHz) **5**, MAO and $Cp_2ZrCl_2$.

measured from the mono-, bi- and tri-component mixtures confirmed the existence of these separate 3-CH–O– molecular fragments. The extended HSQC and HMBC spectra with the characteristic signals marked a–c for the three separate fragments are presented in Fig. 5.

Similarly, the two Cp proton resonances ($\delta$ 5.88 and 6.03 ppm) initially appeared in the ratio 5:1 but later the $^1$H resonance for the pure $Cp_2ZrCl_2$ at $\delta$ 5.88 ppm became barely visible. Hence, the added $Cp_2ZrCl_2$ seems to direct the equilibrium favouring the formation of a certain aluminium alkoxide and simultaneously diminishing the amount of the free alkenol **4** in the tri-component system. The participation of $Cp_2ZrCl_2$ in the observed change in component equilibria is further supported by a weak ROE correlation detected between the *t*-Bu protons ($\delta$ 1.00 ppm) of **4** and the Cp protons at $\delta$ 6.03 ppm. The observed ROE correlation and the shifted $\delta$-value of Cp protons (6.03 ppm, $\Delta\delta_H = 0.15$ ppm compared to $Cp_2ZrCl_2$) suggest a coordination between the comonomer oxygen atom and zirconium in the reaction mixture.

The 1-C$H_3$/2$^1$-C$H_3$ and 3$^1$-C$H_3$/3$^2$-C$H_3$ signals of *t*-alkenol **5** were assigned at $\delta$ 1.03 and 0.85 ppm (Fig. 6(A)). The addition of MAO produced multiple $CH_3$ signals appearing at separate $\delta$ values (Fig. 6(B)). Based on the 2D spectral analysis the different 3$^1$-$CH_3$/3$^2$-$CH_3$ and 1-$CH_3$/2$^1$-$CH_3$ resonances were assigned as being part of three distinct molecular fragments formed in the ratio 1:1:8. The methyl groups exhibited strong ROE correlations to the Al–C$H_3$ signals at $\delta$ −0.22, −0.23 and −0.27 ppm indicating the presence of aluminium alkoxides of which the main component has the chemical shift values of 1.35 (1-C$H_3$/2$^1$-C$H_3$), 0.89 (3$^1$-C$H_3$/3$^2$-C$H_3$) and −0.27 (Al–C$H_3$) ppm.

The addition of $Cp_2ZrCl_2$ into the mixture of **5** and MAO produced few additional signals (Fig. 6(C)) in the $^1$H and $^{13}$C spectra. Based on the 2D spectra, the new proton resonances at $\delta$ 1.23 and 0.81 ppm are part of an aluminium alkoxide absent in the mixture of **5** and MAO. In fact, there existed a weak ROE correlation between the proton signals at $\delta$ 0.81 and −0.40 ppm. However, the connectivities between the other new $^1$H signals appearing at $\delta$ 0.75 and −0.25 ppm could not be deduced from the 2D spectra. Pure $Cp_2ZrCl_2$ ($\delta_H$ 5.88 and $\delta_C$ 116.1 ppm) along with the formed $Cp_2ZrCH_3Cl$ species (Cp $\delta_H$ 5.74, $\delta_C$ 112.9 ppm; $CH_3$ $\delta_H$ 0.36, $\delta_C$ 32.1 ppm) were present in equal amounts. The interaction of zirconocene with MAO could induce the new species observed. In all the studied component

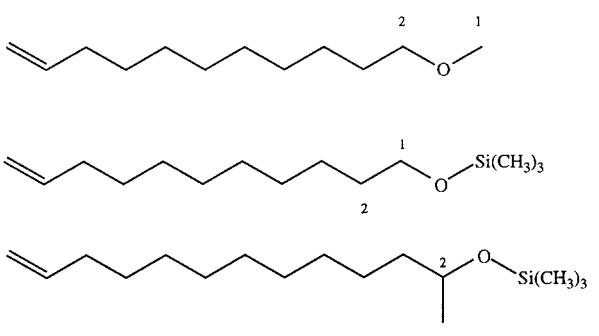


Scheme 3. The structures of (top) 10-undecenyl methyl ether (**6**), (middle) 10-undecenyl trimethylsilyl ether (**7**) and (bottom) 12-tridecen-2-yl trimethylsilyl ether (**8**).

Table 2
Characteristic chemical shift values ($\delta$, ppm) for mono-, bi- and tri-component mixtures of ethers **6**–**8** measured in toluene-$d_8$ [a]

| Compound number | Atomic number | Ether derivative | | Ether derivative with MAO or MAO/$Cp_2ZrCl_2$ | |
|---|---|---|---|---|---|
| | | $^1$H $\delta$ (ppm) | $^{13}$C $\delta$ (ppm) | $^1$H $\delta$ (ppm) | $^{13}$C $\delta$ (ppm) |
| **6** | 1 | 3.16 (s) | 58.3 | 3.15 (s) | 58.3 |
| | 2 | 3.22 (t) | 73.0 | 3.23 (t) | 73.0 |
| **7** | 1 | 3.53 (t) | 62.7 | 3.60 (t) | 65.6 |
| | 2 | 1.52 (m) | 33.3 | 1.56 (m) | 32.4 |
| **8** | 1 | 1.12 (d) | 24.3 | 1.15 (d) | 23.1 |
| | 2 | 3.70 (m) | 68.7 | 3.86 (m) | 71.1 |

[a] Multiplicity (m) of the observed NMR signal is given in parentheses. The atomic number refers to Scheme 3.

mixtures of **5** the $^1$H and $^{13}$C resonances for 12-$CH_2$, 13-CH and 14-$CH_2$ appeared at $\delta$ 2.00, 5.80 and 5.00 ppm and at $\delta$ 34.3, 139.3 and 114.5 ppm, respectively. These resonances did not show HMBC or ROE correlations to the resonances of catalyst system.

### 2.2. Reactions of ether derivatives with the MAO–$Cp_2ZrCl_2$ catalyst system

Based on the 2D spectral analysis, the ether derivatives **6**–**8** (Scheme 3) remained mainly as free comonomers in the presence of MAO. The characteristic $^1$H and $^{13}$C resonances of **6**–**8** in different component mixtures are given in Table 2. For **6** a transient HMBC correlation was found between a $^{13}$C resonance at $\delta_C$ 50.7 ppm ($\delta_H$ 3.10 ppm, s) and a $^1$H singlet at $\delta_H$ $-0.62$ ppm ($\delta_C$ $-10.9$ ppm). Apparently a minor part of **6** existed as a complex with MAO as previously described [16]. Slightly shifted $\delta$ values of 1-*CH*$_2$/2-*CH*$_2$ and 1-*CH*$_3$/2-*CH* were determined for **7** and **8**, respectively. However, these signals did not exhibit HMBC or ROE correlations to the several $^1$H resonances appearing at $\delta$ $-0.35$ to $-0.65$ ppm in the spectrum of **7** or **8** and MAO.

The C*H*$_2$=C*H*–C*H*$_2$ resonances of **6**–**8** were not observed to deviate from their original chemical shift values ($\delta$(H) 5.00, 5.80 and 2.00 ppm) in the presence of MAO. A completely new set of olefinic $^1$H resonances emerged in the spectral region $\delta$ 4.70–5.50 ppm when $Cp_2ZrCl_2$ was added to the mixture of **8** and MAO (Fig. 7). Based on the 2D spectral analysis, these $^1$H signals were assigned to four different fragments with hydrocarbon chains (Scheme 4). The most abundant species formed was the dimer **I**. Three methyl-substituted fragments **II**, **III** and **IV** were present to a lesser extent in the intensity ratio 2:1:1.

Similar behaviour was observed when **7** or 1-undecene were allowed to react with the MAO–$Cp_2ZrCl_2$ catalyst. The former required a reaction time of some weeks in an NMR tube, the latter reacting immediately. Compound **6** did not produce fragments of the types **I**–**IV** even with a prolonged reaction time. Previously, some amino functionalized monomers have been reported to form type **I** dimers in homopolymerizations with borane-activated zirconocene catalysts [28].

### 2.3. Reactions of carbonyl derivatives with the MAO–$Cp_2ZrCl_2$ catalyst system

Slightly altered chemical shift values, $\Delta\delta_H = 0.1$; $\Delta\delta_C = 1.4$ and $\Delta\delta_C = 3.2$, were obtained for 1-*CH*$_3$ and 2-*C*=O resonances of compound **9** (Scheme 5) in the

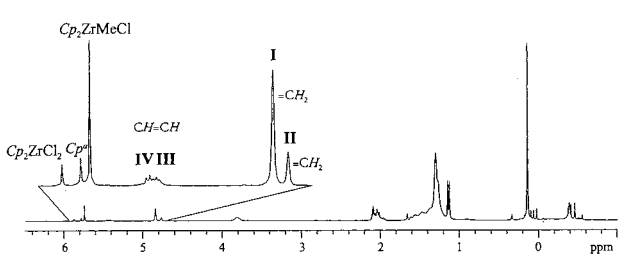


Fig. 7. The $^1$H-NMR spectrum (300 MHz) of **8**, MAO and $Cp_2ZrCl_2$.

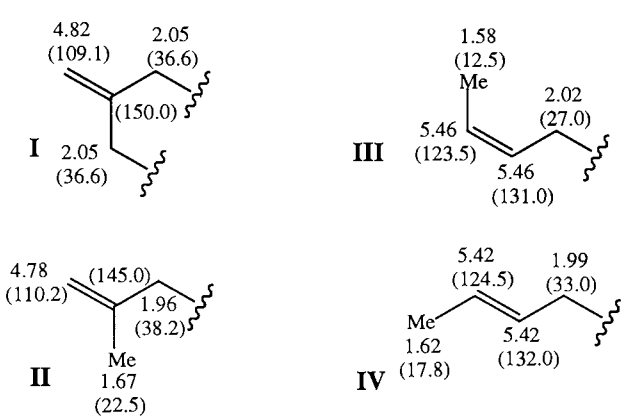


Scheme 4. Structures and chemical $\delta_{H,C}$ values in ppm ($^{13}$C in parentheses) of the four assigned fragments formed in a mixture of **8**, MAO and $Cp_2ZrCl_2$.

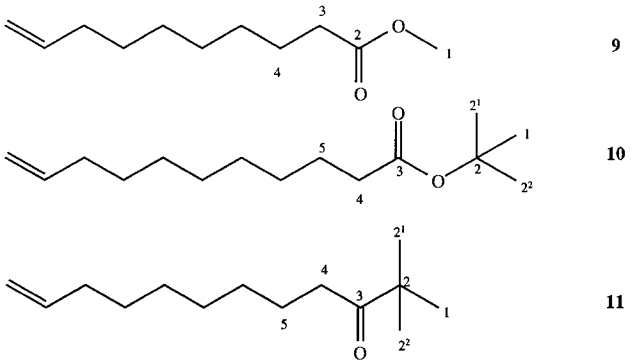

Scheme 5. Structures of the carbonyl derivatives: methyl decenoate (**9**), *t*-butyl undecenoate (**10**) and 2,2-dimethyl-11-dodecen-3-one (**11**).

presence of MAO or MAO/$Cp_2ZrCl_2$ (Table 3). Proton singlets at $\delta$ 3.12 ($\delta_C$ 50.3 ppm) and 3.08 ($\delta_C$ 48.6 ppm) ppm were also observed as well as Al–C$H_3$ resonances at $\delta$ −0.28 to −0.65 ppm ($\delta_C$ −7.0 to −10.0 ppm). $Cp_2Zr(Me)Cl$ and another zirconocene species ($\delta_H$ 5.92 ppm, $\delta_C$ 115.1 ppm) appeared in the tri-component mixture. However, the $^1H$-$^{13}C$ correlations over two or more bonds connecting the observed signals to **9** were not detected.

The other two carbonyl derivatives investigated, *t*-butyl ester **10** and ketone **11** in Scheme 5, produced unsaturated species in their reactions with MAO. An alkene fragment **V** was identified as a reaction product of **10** and MAO (Scheme 6). A partial decomposition of **10** to free 10-undecenoic acid had occurred involving an alkyl–oxygen cleavage to produce a *t*-butyl cation under Lewis acidic conditions. The formed *t*-butyl cation reacts further with MAO through rearrangement(s) and elimination to produce **V**. A coupling constant of 1.1 Hz was measured for the C$H_3$ (d) and C*H* (septet) protons. The $\delta$-values of fragment **V** and a weak NOE correlation detected between the C*H* and Al–C$H_3$ ($\delta$ −0.40 ppm) protons suggest that an aluminium species (AlXMe) is coordinated to **V**.

The addition of $Cp_2ZrCl_2$ did not affect the reaction

Table 3
Characteristic chemical shift values ($\delta$, ppm) for mono-, bi- and tri-component mixtures of carbonyl derivatives **9**–**11** measured in toluene-$d_8$ [a]

| Compound number | Atomic number | $^1H$ $\delta$ (ppm) | $^{13}C$ $\delta$ (ppm) |
|---|---|---|---|
| **9** | 1 | 3.40 (s), [3.30 (s)] | 50.8 [52.2] |
| | 2 | | 173.2 [176.4] |
| | 3 | 2.10 (t) | 34.2 |
| | 4 | 1.50 (m) | 25.3 |
| **10** | 1, $2^1$, $2^2$ | 1.40 (s) | 28.2 |
| | 3 | | 172.3 [173.0] |
| | 4 | 2.10 (t) | 35.7 |
| | 5 | 1.54 (m) | 25.5 |
| **11** | 1, $2^1$, $2^2$ | 0.97 (s) | 26.4 |
| | 3 | | 213.0 |
| | 4 | 2.17 (t) | 36.3 |
| | 5 | 1.56 (m) | 24.3 |

[a] Multiplicity of the observed NMR signal is given in parentheses. The $\delta$ values given in brackets are measured in the presence of MAO or MAO/$Cp_2ZrCl_2$. The numbering of the H and C atoms refers to Scheme 5.

of **10** and MAO noticeably. Monomethyl derivative $Cp_2ZrCH_3(Cl)$ was formed in a ratio 1:1 to $Cp_2ZrCl_2$. Similar to compound **9**, the characteristic $^1H$ and $^{13}C$ signals of unreacted **10** appeared in the NMR spectra measured from the bi- or tri-component mixtures (Table 3).

Two unsaturated fragments with slightly different chemical shift values were formed in a reaction of ketone **11** and MAO in a ratio 1:2 compared to free **11** (Scheme 7). The *t*-Bu, $H^1$ and $H^2$ protons of each fragment exhibited HMBC correlations to the corresponding quaternary carbon atom ($C_q$ at $\delta$ 155.4 or 155.7 ppm). Presumably the oligomeric nature of MAO and the different oxygen–aluminium environments present in MAO solution induced the altered $\delta$ values for the fragment couple. The observed ROE correla-

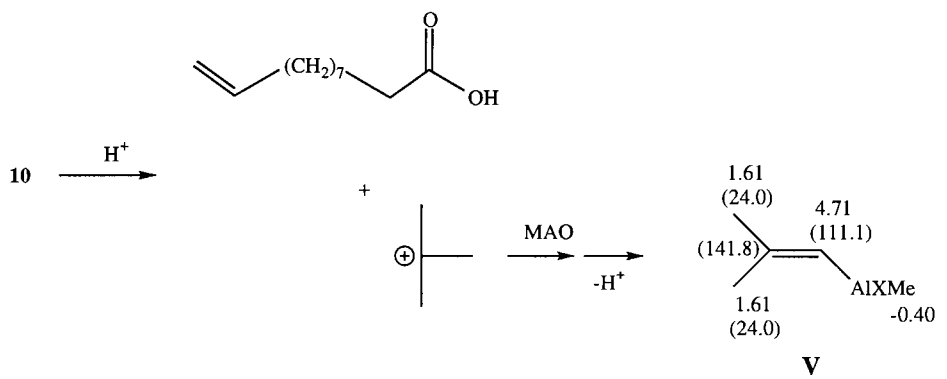

Scheme 6. Chemical $\delta_{H,C}$ values in ppm ($^{13}C$ in parentheses) for fragment **V** identified in a reaction of **10** with MAO (AlXMe = an aluminium species).

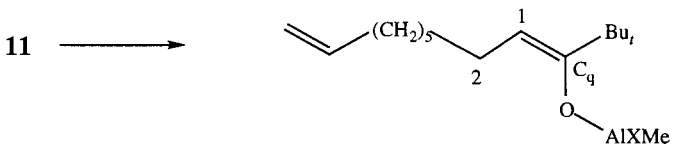


| | δ (ppm) | |
|---|---|---|
| | $^{1}$H | $^{13}$C |
| $^{a}$Bu$_t$ | 1.12 | 29.4 |
| $^{b}$Bu$_t$ | 1.15 | 29.5 |
| $^{a}$C$_q$ | | 155.7 |
| $^{b}$C$_q$ | | 155.4 |
| $^{a}$H$^1$ | 4.83 | 111.0 |
| $^{b}$H$^1$ | 4.87 | 111.6 |
| $^{a}$H$^2$ | 2.16 | 28.1 |
| $^{b}$H$^2$ | 2.25 | 27.9 |

Scheme 7. Chemical $\delta_{H,C}$ values in ppm for the assigned fragments formed in a reaction of **11** with MAO. The superscripts **a** and **b** refer to H and C atoms being part of the same fragment.

tions from the Al–C$H_3$ centred at $\delta$ −0.36 ppm to the $^{b}$H$^1$, $^{b}$H$^2$ and $^{b}t$-Bu protons support this conclusion. Strong ROE correlations between the $t$-Bu ($\delta$ 1.15 and 1.12 ppm) and the methine protons ($\delta$ 4.87 and 4.83 ppm) as well as the absence of the correlation between the $t$-Bu protons and methylene protons ($\delta$ 2.25 and 2.16 ppm) indicate that the formed vinyl ethers exist in the $Z$ configuration (Scheme 7, Fig. 8).

The addition of $Cp_2ZrCl_2$ did not have any immediate observable effect on the product formation. The Cp protons of different zirconocene species appeared at $\delta$ 5.76 ($\delta_C$ 112.5), 5.83 ($\delta_C$ 111.2), 5.88 ($\delta_C$ 115.7) and

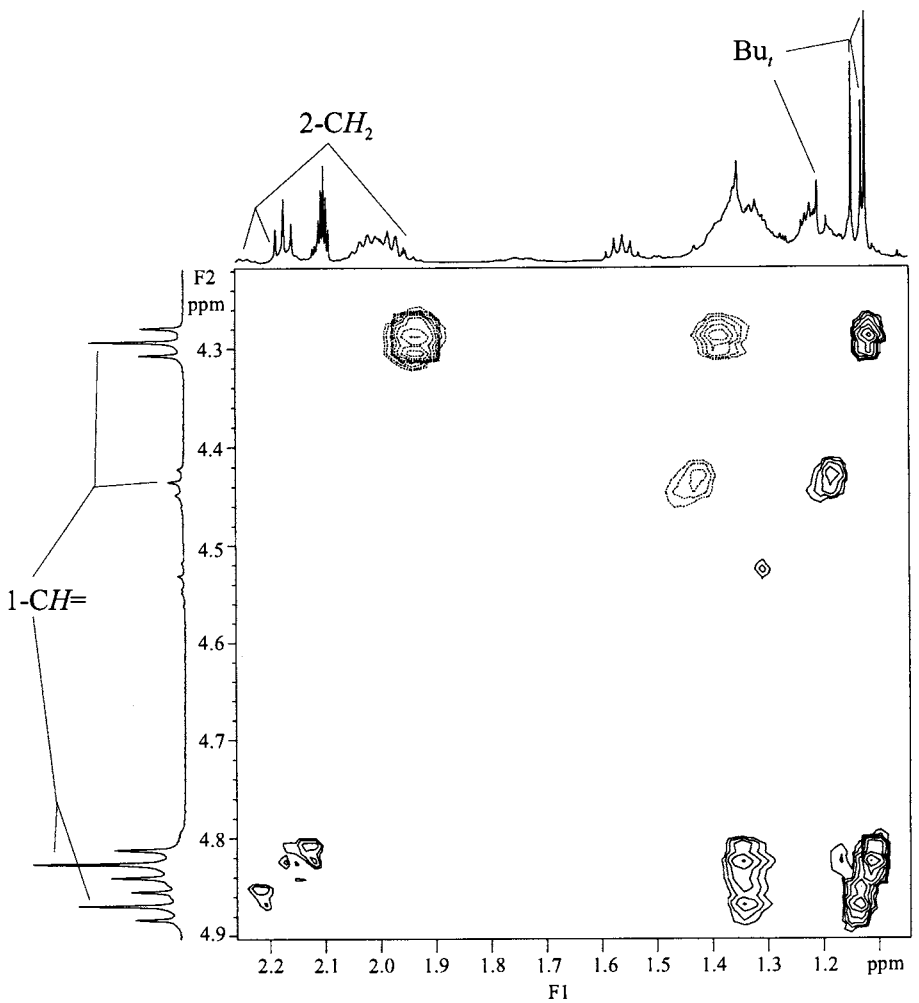


Fig. 8. The expanded ROESY spectrum (500 MHz) of **11**, MAO and $Cp_2ZrCl_2$. The broken line contours are TOCSY and unbroken ROE correlations.

6.03 ($\delta_C$ 114.3) ppm in an equal intensity ratio. The two former Cp signals disappeared and the two latter remained in a ratio 1:10 due to the aging of the NMR sample. Simultaneously, two triplets had emerged at $\delta$ 4.29 and 4.43 ppm in a ratio 8:1. Each of them exhibited a ROE correlation to a new *t*-Bu proton signal at $\delta$ 1.14 or 1.18 ppm, respectively (Fig. 8). The *t*-Bu signals exhibited ROE correlations to the spectral region $\delta$ −0.26 to −0.44 ppm. Accurate $\delta$ values could not be determined due to the overlapping of the corresponding Al–C$H_3$ signals. The lower chemical shift values of the two methine proton resonances (ca. $\Delta\delta$ 0.5 ppm) compared to the original $\delta$ values of $H^1$ reported in Scheme 7 suggest that X is part of a MAO oligomer with an appropriate electronic surrounding to induce the observed shift of $H^1$ protons to a higher field. Presumably the formation of the new unsaturated species has occurred via the zirconocene at $\delta$ 6.03 ppm.

### 2.4. Comparison of the NMR and copolymerization results

The oxygen functionalized alkenes **1**,**3**,**6**–**11** and a *t*-alkenol, 2,2-dimethyl-3-(1,1-dimethylethyl)-11-dodecen-3-ol) synthesized according to the literature [29], have been tested as comonomers in zirconocene–MAO catalysed copolymerizations with ethene or propene [20–23]. The activity of the catalyst system was suppressed to varying degrees depending on the functional group of polar comonomer and the steric hindrance around the hetero atom. The NMR studies suggest that stronger interaction between comonomers and the catalyst system is involved in the case of α- or β-branched rather than straight chain alkenols. In fact, the decomposition of the aluminium alkoxide was observed only for the straight chain alkenol **1**. Presumably the stronger bond or coordination of the Lewis acidic Al to the free electron pair of oxygen reduces the deleterious interactions between a comonomer and active catalyst centres. Moreover, the bond formation between aluminium and comonomer oxygen is not a prerequisite for the diminished catalyst fouling, since equal catalyst activity has been found in copolymerizations of the OMe or OTMS derivatives **6** and **7** compared to **1** [30].

The carbonyl compounds **9**–**11** deactivated the catalyst more strongly than the alkenols or ether derivatives indicating the different interaction of a $CO_2R$ or C=O group with the catalyst system. This deactivation might be caused by the presence of mainly free comonomer in the polymerization reaction, or alternatively by the formation of some other unsaturated species as detected by NMR. The latter were also observed in the $^1$H-NMR spectrum recorded from the copolymerization product of ethene and **10**.

## 3. Experimental

### 3.1. Preparation of MAO and NMR samples

MAO in toluene-$d_8$ (Aldrich 99 + %D) solution (MAO) was prepared from $Al_2(SO_4)_3^*18H_2O$ and TMA according to the standard procedure [24]. The aluminium content of MAO prepared was estimated to be 5.8 wt.%. Its effectivity was tested by homopolymerizing ethene with a zirconocene-based catalyst and comparing the activity with a commercial MAO in toluene solution. The prepared MAO activated the metallocene catalyst as well as the commercial MAO. All NMR samples were prepared under nitrogen in a glove box. The evolution of gas was observed while adding MAO into the toluene-$d_8$ solutions of alkenols **1**–**5.** Consequently, the $^1$H resonance at ca. $\delta$ 0.23 ppm attributable to methane [2] was detected at the spectra measured from the bi- and tri-component mixtures of **1**–**5**. The aforementioned $^1$H signal also appeared at the spectra of **6**–**11** and MAO or MAO/$Cp_2ZrCl_2$. The two- and three-component reaction mixtures in toluene-$d_8$ were studied in 5 mm NMR tubes specially designed for sealing. The tubes were closed with NMR-tube Tip-Off Manifold (Wilmad) and sealed outside the glove box using a butane flame. The sample volumes were 0.7 ml and concentrations of samples were 0.07–0.42 M. In each sample the mole ratio of the alkene derivative and MAO is 1:1 the amount of $Cp_2ZrCl_2$ being catalytic (ca. 5 mg).

### 3.2. Measurement of NMR spectra

The $^1$H and $^{13}$C spectra were referenced to the solvent ($^1$H $\delta$ 2.10 ppm for residual C$H$D$_2$ and $^{13}$C $\delta$ 20.4 ppm resonances of toluene-$d_8$) measured with tetramethylsilane (TMS) added into an unsealed NMR tube. All the samples were measured at 27°C. The $^1$H-, $^{13}$C- and 2D-NMR measurements (HSQC, HMBC, ROESY (or TROESY) and NOESY) were recorded on a Varian Unity 500 MHz (**1**, **4**, **5** and **11**(ROESY)) or a Varian Inova 300 MHz spectrometer (**1**–**11**) using Varian standard pulse sequences. The $^1$H spectra of **2** and **3** were also measured on a Varian Unity 600 MHz. In the HSQC and HMBC experiments the coherence selection was obtained using pulsed field gradients along the *Z* direction. In 2D experiments the data of the indirect dimension were zero filled to be 2 × number of acquired data increments. In phase-sensitive experiments (HSQC, ROESY and NOESY) a $\pi/2$ shifted sine-bell window weighting function were applied in F1 and F2 dimensions. The number of collected transients were 16–64 and time increments 256–512 in 2D experiments. In the ROESY and NOESY 100–200 ms mixing times and acquisition time of 0.18 s were used. In the former, the spin lock was generated using a

DANTE-type pulse sequence. The acquisition times in the HSQC and HMBC were 0.11 and 0.22 s, respectively. In the HMBC experiments, non-shifted sine-bell window weighting functions were used in both dimensions. A relaxation delay of 1 s was used in all experiments.

### 3.3. Origin and spectral data for functionalized alkenes

1-Undecene (received from Fluka) was used as a model compound for a reaction of a non-functionalized alkene with the MAO–$Cp_2ZrCl_2$ catalyst system. The commercial 10-undecen-1-ol **1** was received from Fluka and compound **9** was synthesized by Neste. Compounds **2-5** were synthesized as previously reported [31]. Compounds **6** [32], **7**–**8** [33], **10** [34], and **11** [29] were prepared according to known literature procedures.

Compounds **2**–**11** were purified by the usual chromatographic techniques or vacuum distillation prior to the NMR sample preparation. All the compounds studied were stored under molecular sieves. The following $^1$H- and $^{13}$C-NMR data were recorded for compounds **1**–**11** with a Varian Inova 200 or 300 MHz spectrometer using toluene-$d_8$ as a solvent. Mass spectra as well as high-resolution mass spectra were recorded on a JEOL JMS-SX102 with an EI potential of 70 eV.

Data for compound **1**: $^1$H ($\delta$ ppm): 5.80 (m, 1H), 5.00 (m, 2H), 3.45 (t, 2H), 2.00 (m, 2H), 1.40 (m, 2H), 1.38–1.20 (13H); $^{13}$C ($\delta$ ppm): 139.3, 114.5, 62.7, 34.3, 33.3, 30.2, 30.1, 30.0, 29.7, 29.4, 26.3.

Data for compound **2**: $^1$H ($\delta$ ppm): 5.80 (m, 1H), 5.00 (m, 2H), 3.13 (s, 2H), 2.00 (m, 2H), 1.50–1.10 (15H), 0.83 (s, 6H); $^{13}$C ($\delta$ ppm): 139.3, 114.5, 71.7, 39.2, 35.2, 34.3, 31.2, 30.3, 30.2, 30.1, 29.7, 29.5, 24.4, 24.1; HRMS Calc. for $C_{15}H_{30}O$ 226.2297, Found 226.2299.

Data for compound **3**: $^1$H ($\delta$ ppm): 5.80 (m, 1H), 5.00 (m, 2H), 3.58 (m, 1H), 2.00 (m, 2H), 1.50–1.20 (17H), 1.05 (d, 3H); $^{13}$C ($\delta$ ppm): 139.3, 114.5, 67.7, 39.9, 34.3, 30.3, 30.2, 30.1, 30.0, 29.7, 29.5, 26.3, 23.8; HRMS Calc. for $C_{13}H_{26}O$ 198.1984, Found 198.1988.

Data for compound **4**: $^1$H ($\delta$ ppm): 5.80 (m, 1H), 5.00 (m, 2H), 2.95 (s, 1H), 2.01 (m, 2H), 1.56 and 1.22 (m, 2H), 1.42–1.26 (15H), 1.00 (s, 9H), 0.96 (s, 6H); $^{13}$C ($\delta$ ppm): 139.1, 114.5, 83.7, 42.5, 40.1, 37.6, 34.3, 31.4, 30.3, 30.2, 30.1, 29.7, 29.5, 29.1, 26.0, 25.6, 24.6; HRMS Calc. for $C_{19}H_{38}O$ 282.2923, Found 282.2909.

Data for compound **5**: $^1$H ($\delta$ ppm): 5.80 (m, 1H), 5.00 (m, 2H), 2.00 (m, 2H), 1.44–1.20 (17H), 1.03 (s, 6H), 0.85 (s, 6H); $^{13}$C ($\delta$ ppm): 139.3, 114.5, 74.9, 40.0, 37.4, 34.3, 31.5, 30.4, 30.3, 30.1, 29.7, 29.5, 25.6, 25.3, 21.6; HRMS Calc. for $C_{17}H_{34}O$ 254.2609, Found 254.2599.

Data for compound **6**: $^1$H ($\delta$ ppm): 5.80 (m, 1H), 5.00 (m, 2H), 3.22 (t, 2H), 3.16 (s, 3H), 2.00 (m, 2H), 1.52 (m, 2H), 1.42–1.16 (12H); $^{13}$C ($\delta$ ppm): 139.3, 114.5, 73.0, 58.3, 34.3, 30.3, 30.1, 30.0, 29.9, 29.6, 29.4, 26.7; HRMS Calc. for $C_{12}H_{24}O$ 184.1827, Found 184.1823.

Data for compound **7**: $^1$H ($\delta$ ppm): 5.80 (m, 1H), 5.00 (m, 2H), 3.53 (t, 2H), 1.98 (m, 2H), 1.52 (m, 2H), 1.42–1.16 (10H), 0.12 (s, 9H); $^{13}$C ($\delta$ ppm): 139.3, 114.5, 62.7, 38.3, 34.3, 33.3, 30.1, 30.0, 29.6, 29.4, 26.4,–0.38; HRMS Calc. for $C_{14}H_{30}OSi$ 242.2066, Found 242.2055.

Data for compound **8**: $^1$H ($\delta$ ppm): 5.80 (m, 1H), 5.00 (m, 2H), 3.70 (m, 1H), 2.00 (m, 2H), 1.50–1.20 (16H), 1.12 (d, 3H), 0.14 (s, 9H); $^{13}$C ($\delta$ ppm): 139.3, 114.5, 68.7, 40.2, 34.3, 30.3, 30.2, 30.1, 30.0, 29.7, 29.5, 26.4, 24.3, 0.43; EI (70 eV): $m/z$ 170.

Data for compound **9**: $^1$H ($\delta$ ppm): 5.75 (m,1H), 5.00 (m, 2H), 3.40 (s, 3H), 2.10 (t, 2H), 1.94 (m, 2H), 1.50 (m, 2H), 1.32–1.10 (8H); $^{13}$C ($\delta$ ppm): 173.2, 139.2, 114.5, 50.8, 34.2, 34.1, 29.6, 29.5, 29.4, 29.3, 25.3.

Data for compound **10**: $^1$H ($\delta$ ppm): 5.80 (m, 1H), 5.00 (m, 2H), 2.10 (t, 2H), 1.97 (m, 2H), 1.54 (m, 2H), 1.40 (s, 9H), 1.36–1.14 (10H); $^{13}$C ($\delta$ ppm): 172.3, 139.2, 114.5, 79.2, 35.7, 34.3, 29.8, 29.7, 29.5, 29.4, 28.2, 25.5; EI (70 eV): $m/z$ 240.

Data for compound **11**: $^1$H ($\delta$ ppm): 5.77 (m, 1H), 5.00 (m, 2H), 2.17 (t, 2H), 1.98 (m, 2H), 1.56 (m, 2H), 1.40–1.10 (10H), 0.97 (s, 9H); $^{13}$C ($\delta$ ppm): 213.0, 139.2, 114.5, 43.8, 36.3, 34.2, 29.9, 29.7, 29.5, 29.4, 26.4, 24.3; HRMS Calc. for $C_{14}H_{26}O$ 210.1984, Found 210.1993.

## 4. Conclusions

Based on the $^1$H- and $^{13}$C-NMR measurements including HSQC, HMBC, ROESY and NOESY experiments, interaction mechanism(s) between an oxygen functionalized alkene with an MAO–$Cp_2ZrCl_2$ catalyst exhibited a clear dependence on the nature of the functional group and on the steric hindrance around the hetero atom. Hydroxyl functionalized alkenes **1**–**5** formed alkoxides with MAO even in the presence of $C(CH_3)_3$ and $C(CH_3)_2$ groups $\alpha$ to the OH group. On the contrary, their OMe or TMS derivatives (**6**–**8**) remained mainly as free comonomers in the presence of MAO. For compound **6** an HMBC correlation indicating a partial coordination to MAO was detected. $\alpha$- or $\beta$-branching to the OH group of an alkenol induced the formation of several aluminium alkoxides. On the other hand, the highly sterically hindered **4** and the straight chain alkenol **1** formed one main species with MAO. Apparently a moderate degree of branching allows the formation of aluminium alkoxides from structurally different MAO oligomers.

Zirconocene seemed to enhance the interaction between an alkenol and MAO since additional aluminium

alkoxides were detected in the tri-component mixtures. A more pronounced effect of zirconocene was observed in the reaction of TMS derivative **8** which produced dimers of the type $CH_2{=}CR_1R_2$ along with methylated derivatives $CH_2{=}C(Me)(R)$ and $(Me)CH{=}CH(R)$ (R, $R_1$, $R_2$ = hydrocarbon chain) with the catalyst system. Compound **7** and 1-undecene reacted analogously, the former being the least reactive.

Compound **10** was partly decomposed to $Me_2C{=}CH{-}Al{-}X$ species in its reaction with MAO or $MAO/Cp_2ZrCl_2$. Two unsaturated $CH_2{=}CH(CH_2)_5CH_2CH{=}C(t\text{-}Bu)O{-}Al(CH_3){-}X$ species with slightly different chemical shift values were assigned in the reaction of ketone **11** with MAO. Additional similar fragments emerged in the tri-component mixture of **11**. Obviously the characteristic $^1H$ and $^{13}C$ resonances of the four fragments appear at different $\delta$ values due to the X being part of a different MAO oligomer.

In all the studied tri-component mixtures the olefinic part of comonomers were found not to interact directly with $Cp_2ZrCl_2$ or other zirconocene species formed in the component mixture. An ROE correlation between the olefinic protons of *sec* alkenol **3** or **4** and methyl protons of MAO was observed, suggesting coordination of the C=C of **3** or **4** to MAO. A more precise structure could not be deduced on the basis of the measured spectra. The nature of interaction appears to be rather weak since the chemical shift values for $CH_2{=}CH$ did not alter compared to the corresponding $\delta_H$ values of free **3** or **4**. Hence, only limited information about the structure of aluminium fragments coordinated or attached to comonomers could be obtained by the utilized solution NMR techniques. By comparing ROESY with NOESY measurements, the observed ROE correlations were always detected as NOEs with positive signs. Thus the molecular weights of formed species were clearly below 1000 g $mol^{-1}$ based on the molecular correlation times [35].

## Acknowledgements

This work was supported by the Neste Foundation.

## References

[1] E. Giannetti, G.M. Nicoletti, R. Mazzochhi, J. Polym. Sci. Polym. Chem. Ed. 23 (1985) 2117.
[2] L. Resconi, S. Bossi, L. Abis, Macromolecules 23 (1990) 4489.
[3] A.R. Siedle, W.M. Lamanna, J.M. Olofson, B.A. Nerad, R.A. Newmark, ACS Symp. Ser. 517 (1993) 156.
[4] I. Tritto, M.C. Sacchi, P. Locatelli, S.X. Li, Macromol. Chem. Phys. 197 (1996) 1537.
[5] I. Tritto, C. Mealares, M.C. Sacchi, P. Locatelli, Macromol. Chem. Phys. 198 (1997) 3963.
[6] D.E. Babushkin, N.V. Semikolenova, V.N. Panchenko, A.P. Sobolev, V.A. Zakharov, E.P. Talsi, Macromol. Chem. Phys. 198 (1997) 3845.
[7] M.R. Mason, J.M. Smith, S.G. Bott, A.R. Barron, J. Am. Chem. Soc. 115 (1993) 4971.
[8] W. Kaminsky, A. Bark, R. Steiger, J. Mol. Catal. 74 (1992) 109.
[9] W. Kaminsky, R. Steiger, Polyhedron 7 (1988) 2375.
[10] A.R. Siedle, R.A. Newmark, W.M. Lamanna, J.N. Schroepfer, Polyhedron 9 (1990) 301.
[11] D. Cam, U. Giannini, Makromol. Chem. 193 (1992) 1049.
[12] I. Tritto, R. Donetti, M.C. Sacchi, P. Locatelli, G. Zannoni, Macromolecules 30 (1997) 1247.
[13] P.G. Gassman, M.R. Callstrom, J. Am. Chem. Soc. 114 (1987) 7875.
[14] C. Sishta, R.M. Hathorn, T.J. Marks, J. Am. Chem. Soc. 114 (1992) 1112.
[15] C.J. Harlan, S.G. Bott, A.R. Barron, J. Am. Chem. Soc. 117 (1995) 6465.
[16] S. Pasynkiewicz, Polyhedron 9 (1990) 429.
[17] Y. Koide, S.G. Bott, A.R. Barron, Organometallics 15 (1996) 5514.
[18] C.E. Bethley, C.L. Aitken, C.J. Harlan, Y. Koide, S.G. Bott, A.R. Barron, Organometallics 16 (1997) 329.
[19] J. Turunen, T.T. Pakkanen, B. Löfgren, J. Mol. Cat. A: Chem. 123 (1997) 35.
[20] P. Aaltonen, B. Löfgren, Macromolecules 28 (1995) 5353.
[21] P. Aaltonen, G. Fink, B. Löfgren, J. Seppälä, Macromolecules 29 (1996) 5255.
[22] P. Aaltonen, B. Löfgren, Eur. Polym. J. 33 (1997) 1187.
[23] K. Hakala, B. Löfgren, T. Helaja, Eur. Polym. J. 34 (1998) 1093.
[24] D. Cam, E. Albizzati, P. Cinquina, Makromol. Chem. 191 (1990) 1641.
[25] J.H. Rogers, A.W. Apblett, W.M. Cleaver, A.N. Tyler, A.R. Barron, J. Chem. Soc. Dalton Trans. (1992) 3179.
[26] Z. Wu, R.F. Jordan, J.L. Petersen, J. Am. Chem. Soc. 117 (1995) 5867.
[27] R.F. Jordan, C.S. Bajgur, W.E. Dasher, A.L. Rheingold, Organometallics 6 (1987) 1041.
[28] U.M. Stehling, K.M. Stein, M.R. Kesti, R.M. Waymouth, Macromolecules 31 (1998) 2019.
[29] P.J. Pearce, D.H. Richards, N.F. Scilly, Org. Synth. 52 (1972) 19.
[30] K. Hakala, B. Löfgren, T. Helaja, in preparation.
[31] T. Helaja, B. Löfgren, T. Hase, Acta Chem. Scand., in press.
[32] R.A.W. Johnstone, M.E. Rose, Tetrahedron 35 (1979) 2169.
[33] H. Adlercreutz, T. Fotsis, C. Bannwart, K. Wähälä, G. Brunow, T. Hase, Clin. Chim. Acta 199 (1991) 263.
[34] S. Ohta, A. Shimabayashi, M. Aono, M. Okamoto, Synth. Commun. (1982) 833.
[35] H. Günther, NMR Spectroscopy. Basic Principles, Concepts, and Applications in Chemistry, 2nd edn, Wiley, Chichester, 1995, p. 403.